NeuroImage 248 (2022) 118839

Contents lists available at ScienceDirect

NeuroImage

journal homepage: www.elsevier.com/locate/neuroimage

Motor impairment evoked by direct electrical stimulation of human parietal cortex during object manipulation

Luca Fornia [a,c], Marco Rossi [b], Marco Rabuffetti [c], Andrea Bellacicca [a], Luca Viganò [b], Luciano Simone [d], Henrietta Howells [a], Guglielmo Puglisi [a], Antonella Leonetti [a], Vincenzo Callipo [e], Lorenzo Bello [b], Gabriella Cerri [e,*]

[a] Laboratory of Motor Control, Department of Medical Biotechnologies and Translational Medicine, Università degli Studi di Milano, Italy
[b] Neurosurgical Oncology Unit, Department of Oncology and Hemato-Oncology, Università degli Studi di Milano, Italy
[c] IRCCS Fondazione Don Carlo Gnocchi, Milano, Italy
[d] Cognition, Motion & Neuroscience, Center for Human Technologies, Istituto Italiano di Tecnologia, Genoa, Italy
[e] Laboratory of Motor Control, Department of Medical Biotechnologies and Translational Medicine, Università degli Studi di Milano, Humanitas Research Hospital IRCSS, Rozzano, Milano, Italy

ARTICLE INFO

Keywords:
Human Parietal cortex
motor control
hand-manipulation
EMG
intraoperative stimulation

ABSTRACT

In primates, the parietal cortex plays a crucial role in hand-object manipulation. However, its involvement in object manipulation and related hand-muscle control has never been investigated in humans with a direct and focal electrophysiological approach. To this aim, during awake surgery for brain tumors, we studied the impact of direct electrical stimulation (DES) of parietal lobe on hand-muscles during a hand-manipulation task (HMt). Results showed that DES applied to fingers-representation of postcentral gyrus (PCG) and anterior intraparietal cortex (aIPC) impaired HMt execution. Different types of EMG-interference patterns were observed ranging from a partial (task-clumsy) or complete (task-arrest) impairment of muscles activity. Within PCG both patterns coexisted along a medio (arrest)–lateral (clumsy) distribution, while aIPC hosted preferentially the task-arrest. The interference patterns were mainly associated to muscles suppression, more pronounced in aIPC with respect to PCG. Moreover, within PCG were observed patterns with different level of muscle recruitment, not reported in the aIPC. Overall, EMG-interference patterns and their probabilistic distribution suggested the presence of different functional parietal sectors, possibly playing different roles in hand-muscle control during manipulation. We hypothesized that task-arrest, compared to clumsy patterns, might suggest the existence of parietal sectors more closely implicated in shaping the motor output.

1. Introduction

Refined control of extrinsic and intrinsic hand muscles is crucial to achieve a correct hand-object interaction. In this regard, premotor areas have been shown to be crucial in shaping hand-muscles for goal directed movements both in human and non-human primate (Davare et al., 2008, 2009; Baumer et al., 2009; Fornia et al., 2020a; Cerri et al., 2003; Prabhu et al., 2009; Cotè et al., 2017).

However, although the precise shaping of muscle contraction during object manipulation is historically related to frontal motor areas, several studies in both non-human and human primates, suggest that also anterior and posterior parietal areas are potentially involved in control of hand-muscle during skilled action.

In this regard, in non-human primates it has been shown that specific parietal hand-related sectors act on motor output via their crucial connections with distinct motor and premotor sectors (Stepniewska et al., 2014; Gharbawie et al., 2011). In particular, within postcentral gyrus, area 3a, 1, 2 are densely interconnected with primary motor cortex (Kaneko et al. 1994), while within the posterior parietal areas specific connections between anterior intraparietal (AIP) and ventral premotor (vPM, F5) areas are crucial nodes of a large-scale cortical network functionally specialized in controlling hand movements (Borra et al., 2017). In addition, Rathelot and coworkers showed that lateral area 5 (PEip and PE) is source of di-synaptic corticospinal projections terminating on last-order interneurons in the dorsal horns (Rathelot et al., 2017) allowing a more direct control of spinal motoneurons with respect to the more indirect control exerted via connections with frontal motor areas. Corticospinal projections has been shown also from other parietal sectors including area 1, 2, anterior intraparietal and inferior parietal areas (Nudo et al., 1990; Rozzi et al., 2006; Innocenti et al., 2019),

* Corresponding author.
E-mail address: gabriella.cerri@unimi.it (G. Cerri).

https://doi.org/10.1016/j.neuroimage.2021.118839.
Received 2 July 2021; Received in revised form 3 December 2021; Accepted 18 December 2021
Available online 25 December 2021.

although without evidence of their spinal targets. Overall, non-human primates' data suggested that the anterior and posterior parietal cortex contribute to hand-muscles control during dexterous action, possibly via direct (cortico-spinal) or indirect (parieto-frontal) action on spinal circuits.

In humans, most of the studies investigating the role of the parietal lobe in object manipulation and relative hand-muscle control comes from non-invasive techniques. The fMRI studies has shown a wide spread activation in the parietal areas during grasping and object manipulation tasks, including postcentral gyrus, superior parietal lobe, anterior and middle intraparietal sulcus (Konen et al. 2013; Gallivan & Culham 2015; Errante et al., 2021). The causal functional relationship between these parietal sectors and the motor output has been investigated with different TMS methods. Davare and collaborators reported that repetitive TMS over anterior intraparietal area (AIP) impairs hand shaping and force scaling during visuo-guided grasping and lifting task (Davare et al., 2007). Koch and collaborators, by using a TMS conditioning test at rest, showed that single pulse in the anterior and caudal posterior parietal cortex modulate differently the excitability of ipsilateral hand-knob region in primary motor cortex and its related hand-muscle evoked response (Koch et al., 2007). A conditioning-test study during reaching-grasping movements reported a facilitation of the primary motor output by AIP stimulation specifically during grip formation (Vesia et al. 2013). TMS has been used also on anterior postcentral gyrus (hand region of primary somatosensory cortex) to interfere with grasping and object manipulation, reporting an effect on control of load forces (Parikh et al. 2020) and of coordination between object contact and the subsequent lifting (Schabrun et al. 2008).

In spite of this evidence, the involvement of human anterior and posterior parietal sectors in hand-object manipulation and its related muscles control has never been investigated with a focal and direct electrophysiological approach. In this regard, interesting insights may come from intraoperative studies using direct electrical stimulation (DES) and simultaneous muscle recording (Fornia et al 2020; Viganò et al., 2021). Although the physiological mechanism underlying the DES needs to be clarified (Borchers et al., 2011) and its application is constrained by clinical needs, this technique has proved to be an efficient tool to study neural functions including motor behavior (Desmurget et al., 2015). Moreover, DES represents a direct electrophysiological approach similar, although not equivalent, to that applied in non-human primates. This aspect is crucial to allow a more reliable comparison between human and non-human electrophysiological data, in a perspective of functional homology and is mandatory in light of the huge expansions of the human neocortex compared to non-human primate (Van Essen et al. 2016).

In a previous study (Fornia et al., 2020), we used the DES in awake patients to investigate the role of premotor areas in shaping muscle activity during an ecological motor task requiring an haptically driven hand-object interaction (i.e. hand-manipulation task, HMt). The HMt consists of a cylindrical handle fixed close to the patient's hand along the armrest of the operating table. Patients were trained to haptically grasp (without visual feedback), hold, rotate, and release the cylindrical handle continuously with a self-paced rhythmicity. The grip required the opposition between the thumb and the index finger, resembling as possible a precision grip. The proximity between the hand and the cylindrical handle allowed the patients to perform the movement using just the hand and the fingers, avoiding any reaching movements (Fig. 1A). Other intraoperative studies investigated hand-arm movements, although stimulating during the performance of a non-object related task, such as hand opening/closing (Rech et al., 2019; Desmurget et al. 2018), which requires a lower level of dexterity with respect to the HMt. The requirement of the object manipulation represents an important aspect in common (although absolutely not strictly comparable) with fMRI and TMS tasks adopted for investigating the parieto-frontal pathways involved in object manipulation movements (Gallivan & Culham, 2015; Errante et al., 2021; Nelissen & VanDuffell 2011; Koch & Rothwell 2009).

In this context, our data showed that long trains (2-4 s) of bipolar 60Hz DES (low frequency DES; LF-DES) applied over premotor areas fails to evoke motor responses in the upper limb of patients at rest, obtained conversely, with monopolar high frequency DES (HF-DES) (Fornia et al. 2018). However, when LF-DES was applied over specific sector of premotor cortex during the HMt execution, it affected the hand-object interaction and the correct hand-muscle activity evoking different muscle-related interference patterns (Fornia et al. 2020). The different hand-muscles patterns evoked by LF-DES during HMt in ventral and dorsal premotor areas pointed to different functional relationship of the ventral and dorsal premotor areas with neural substrates responsible for shaping hand-muscle during voluntary motor output. This hypothesis was confirmed by investigating the functional resting state connectivity of the different premotor sectors intraoperatively identified (Simone et al., 2020). Despite a similar functional connectivity pattern between ventral and dorsal premotor area, the former showed a stronger functional connectivity with a bilateral set of parieto-frontal areas involved in the hand-related sensorimotor process, while the latter with primary somatomotor regions organized around the hand-knob region (Simone et al., 2021). Based on previous results, the primary aim of this study was to assess, by means of LF-DES, the involvement of the parietal lobe in object manipulation and its related hand-muscle control. Should this be the case, LF-DES is expected to disrupt HMt ongoing execution and the related hand-muscles activity only when applied on parietal sectors functionally involved in task execution by shaping the motor output to muscles and/or the flow of sensorimotor integration. A lack of effect on HMt execution and its hand-muscle activity would reflect the stimulation of a parietal sector not primarily involved neither in shaping the motor output to muscles nor in the sensorimotor integration required by task. Moreover, we speculated that possible different effects on hand-muscles evoked by parietal LF-DES might reflect the recruitment of different pathways eventually affecting the excitability of motor output to muscles.

2. Materials and methods

2.1. Patient selection and inclusion criteria

Candidates were right-handed patients affected by a glioma in the left hemisphere requiring the complete or the partial exposure of the parietal lobe. Neuroradiological inclusion criteria were applied irrespective of tumor location, based on an extensive and multidisciplinary preoperative evaluation involving standard MR studies (T1, FLAIR and DWI) (Philips Intera 3T scanner, Best). Patients with tumor occupying more than 10 cc of the parietal lobe, were not included. Patients who received previous neurosurgical treatment and/or patients that showed preoperative sensorimotor and/or praxis deficits were not included. Sensorimotor deficits were assessed by means of standard neurological examination and Action Research Arm Test (ARAT) test, while upper limb apraxia has been assessed by means of De Renzi test. All patients gave written informed consent to the surgical and mapping procedure and to use of data for research purposes, which followed the principles outlined in the "World Medical Association Declaration of Helsinki: Research involving human subjects". The study was performed with strict adherence to the routine procedure normally utilized for surgical tumor removal.

Finally, thirty-four right-handed patients were enrolled in this study (mean age 46 ± 12.5 SD, range 25-75, $n = 19$ with high-grade glioma; $n = 14$ with low-grade glioma, $n = 1$ others). Selected patients showed a normal score for the upper limb apraxia (De Renzi test), no basic sensory and motor deficits (neurological examination) and scored 57 (the highest score) in the Action Research Arm test (ARAT). Among them, in 20 patients the tumor was growing in parietal areas (mean volume of 9.79cc ± 8.2), in 8 patients in the frontal lobe not infiltrating the precentral gyrus (mean volume 11.95cc ± 8.47) and in 6 patients in the temporal lobe (mean volume 16.8cc ± 5.68). The main aim of the study was to investigate the parietal lobe and, due to the surgical approach,

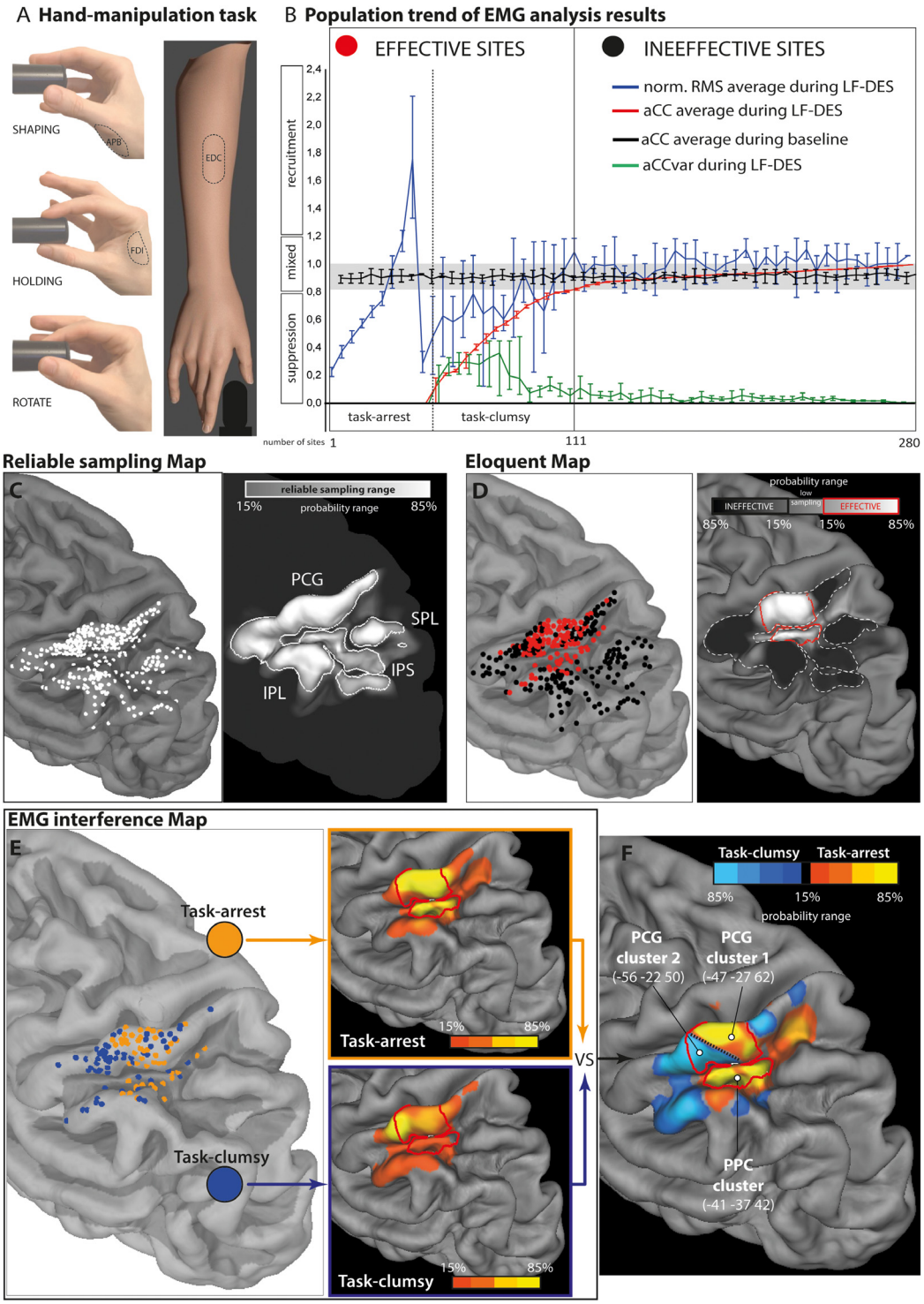

Fig. 1. (A) Schematic representation of hand-manipulation task, side and top view showing the different phases of the task, the overall arm-hand position during task and the muscles analyzed (**B) Population trend of EMG analysis (aCC and RMS) results in the 280 sites**. Red line represents the aCC average value computed on EMG ongoing activity during stimulation of each site; the black line represents the aCC average value computed on EMG ongoing activity during baseline HMt execution and the green dashed line represents mean aCC variation for each site. Aligned with aCC-related parameters, the blue line represents the average RMS normalized value recorded from each site. The results were ranked from the lowest to the highest aCC average value corresponding to stimulated sites (indicated as numbers on x axis). The RMS normalized value is represented following the exact ranking order adopted for the aCC average, allowing a direct comparison of the parameters. In order to show all the trend of stimulated sites ($n = 280$) in the figure. For graphical reason each graph-point represents the average from 5 sites and the whiskers indicates the related standard deviation. On the axes are indicated the corresponding different types of EMG interference patterns (Task-arrest vs –clumsy on x axes) and muscle effects (suppression, mixed and recruitment on y axes). (C) **Reliable sampling map** shows the overall stimulated sites (white dots) and the corresponding probability density estimation. **(D) Eloquent map** (in red effective sites, in black ineffective sites) and results of the subtraction between effective and ineffective probability density showing the main eloquent parietal area within the red border. **(E) EMG-interference map** shows the distribution of task-arrest (gold) and task-clumsy patterns (blue) and their corresponding probability density estimation. In **(F)** the overall results of the subtractions between task-arrest and -clumsy probabilities maps and related clusters within the eloquent parietal map. For each cluster, the MNI coordinates of the center of mass is indicated. (For interpretation of the references to color in this figure legend, the reader is referred to the web version of this article).

the most extensive exploration was allowed mainly when the tumor was located within the parietal white matter. In order to overcome as much as possible the effects due to the presence of the tumor within the investigated area, we selected patients with a parietal tumor volume not exceeding the 10 cc. Only two patients exceeding this value were included, since their responses fitted spatially with the overall stimulation sample of effective sites. Among frontal and temporal tumors, we selected patients requiring, for clinical need, to have the postcentral gyrus and/or the inferior parietal lobe exposed and to execute HMt.

2.2. Intraoperative procedure

Total intravenous anesthesia with Propofol and Remifentanil was used, and no muscle relaxants were employed during surgery to allow mapping of motor responses. A craniotomy was performed to expose the tumor area and a limited amount of surrounding tissue. Surgery was performed in all patients under asleep-awake-asleep anesthesia, with the aid of the neurophysiological Brain Mapping and Monitoring techniques (Bello et al. 2014). The resection was stopped according to functional boundaries, preserving motor, praxis, language, visual and cognitive functions (Conti Nibali et al., 2020, Rossi et al. 2021, 2021, 2018).

2.3. Neurophysiological brain mapping

To perform brain mapping, two stimulation techniques were available to the surgeon: Low Frequency (LF-DES) and High Frequency (HF-DES) protocol (Bello et al. 2014; Rossi et al., 2019). The present study has been performed by using the LF-DES consisting of trains, lasting 2 to 5 s, of biphasic square wave pulses (0.5 ms each phase) at 60 Hz (ISI 16.6 ms) delivered at variable intensity (intensity range 2-6 mA) by a constant current stimulator (OSIRIS-NeuroStimulator, Inomed) integrated into the ISIS-System through a bipolar probe (2 ball tips, 2 mm diameter, separation 5 mm. In all patients considered for this study, the LF-DES was used first, during language mapping and then during the Hand-Manipulation task.

2.4. Hand-manipulation task (HMt)

The same intensity adopted for language assessment was used during HMt. A specific tool was made for this specific purpose. It consists of a small cylindrical handle (Ø 2 and length 6 cm) inserted inside a fixed rectangular base (3 × 3 cm and 9 cm of length) by means of a worm-screw. The rectangular base was kept stable close to the patient's hand along the armrest of the operating table, while the patient sequentially grasped, held, rotated, and released the cylindrical handle continuously with the thumb and the index finger, using a precision grip. The proximity between the hand and the cylindrical handle allowed the patients to perform the movement using just the fingers, avoiding any reaching movements (Fornia et al., 2020; Rossi et al., 2018; see Fig. 1A). Each patient was opportunely trained the day before surgery to perform the HMt at and to report any perceived task-related difficulties, including somatic sensation possibly evoked by LF-DES. The task was performed with the highest regularity paced by an internally generated rhythm (frequency rate of about 0.5 Hz each cycle; grasp, hold, rotate and back to grasp), without any external cue or visual information about the hand or the cylindrical handle movement. During the procedure, a trained neuropsychologist performed real-time monitoring of the patients' HMt behavioral outcome, reporting any impairment in task performance and/or any somatic sensation reported by patients. In order to achieve the main aim of the study, an offline analysis of the EMG data recorded during HMt execution was performed. To this aim, out of the 24 muscles simultaneously recorded in the clinical setting (bilateral Orbicularis Oris, bilateral Biceps Brachii, bilateral Triceps Brachii, bilateral Extensor Digitorum Communis, bilateral Abductor Pollicis Brevis, bilateral Abductor Digiti Minimi, bilateral First Dorsal Interosseous, contralateral Mylohyoid, Mentalis Quadriceps, Hamstring, Tibialis Anterior, Triceps Surae, Flexos Allucis Brevis), the activity of the right Abductor Pollicis Brevis (APB), the First Dorsal Interosseous (FDI) and the Extensor Digitorum Communis (EDC) was selected for the analysis. These muscles were selected since, among the muscles routinely recorded in this clinical setting, they were the most active prime movers in HMt execution. However, all the 24 muscles were visually inspected during analysis in order to qualitatively check the occurrence of effects also in muscles not primarily involved by the task, such as upper-limb proximal, oro-facial, lower-limb muscles. During surgery, the ongoing hand-object interaction was video recorded with the EMG signal, the video of the surgical flap and the DES onset/offset. At the beginning of the HMt session, the patient was asked to start the performance at his/her own rhythm to achieve a rhythmic, regular and stable task execution, assessed by online inspection of the behavioral outcome and of the ongoing EMG activity. Once this condition was achieved, LF-DES stimulation of the cortical areas of interest was delivered, randomly during HMt execution, by the surgeon (L.B. and M.R.). Stimulations were spaced by 3-4 s to avoid dragging effects. When LF-DES interfered with the HMt execution, an extra time of 3-4 sec was given to the patient to regain regular performance and to continue the procedure.

2.5. Data analysis

In order to investigate the effect of LF-DES delivered on different parietal sectors during HMt execution, the intraoperative EMG data recorded was extracted and offline analyzed as follows.

2.5.1. EMG analysis: recording, selection and pre-processing of the EMG signal

In compliance with the clinical procedure, the EMG activity of all muscles, including the muscles selected for the study, was recorded during HMt (ISIS, INOMED, sampling rate 2000 Hz, notch filter at 50 Hz). This data was further analyzed offline. For each patient, the raw data was extracted and analyzed with a dedicated software (MatLab, Math Works 2018b) allowing for selection of specific epochs related to HMt execution without (baseline) and with LF-DES. Baseline HMt execution was assessed by selecting three subsequent epochs (3 s each one) of EMG activity within the initial baseline, than, for each LF-DES trial during HMt execution we selected the time window between stimulation onset and offset. Onset and offset of stimulation was selected by using the stimulation-related artefact from an electrode routinely placed on the forehead (close to the orbicularis oculi muscle) and recorded by one of the EMG synchronized-channels. The quantitative analysis of EMG signal was selectively performed on the Extensor Digitorum Communis (EDC), First Dorsal Interosseous (FDI) and Abductor Pollicis Brevis (APB). The selected EMG was low pass filtered at 500 Hz and multiple notch filters from 60 to 480 Hz were applied to remove LF-DES artifacts and its harmonics. In the analysis, following a careful offline inspection of the video regarding patient's performance during intraoperative mapping, we excluded data recorded during stimulation trials when LF-DES-unrelated problems were reported.

2.5.2. Parameters calculated on EMG

Two quantitative parameters were calculated on the EMG in each muscle across the different conditions, i.e. all the stimulations (Effective and Ineffective) and the baseline. 1) **Autocorrelation coefficient** (aCC), was computed, in each patient, on all the EMG time window selected (i.e. Baseline and LF-DES-related) for each muscle. Specifically, the autocorrelation analysis (Matlab function "xcorr", using the "unbiased" option) was applied on each EMG window selected, after being demeaned, full-wave rectified and low-pass-filtered; the resulting autocorrelation function, when a phasic activity was maintained, was characterised by a prominent positive peak whose timing corresponded to the fundamental time period (f0), inverse of the fundamental frequency (Nelso-Wong et al., 2009); the y-value of this peak was the aCC index

accounting for the regularity/rhythmicity of the phasic muscle contraction during HMt execution. The closer to the unitary value the peak aCC index is, the more repeatable and regular is to be considered the EMG pattern. Therefore, the values of aCC close to 1 accounted for the adequate activation (phasic) in time of muscles contraction during HMt execution. When, due to a missing repetitive pattern, no prominent positive peak was identified on the autocorrelation function, the aCC was given a null value (aCC=0), while when the repetitive activation pattern was partially disrupted, the prominent peak lowers and so the aCC does. In the analysis, we first quantified the overall patient's muscle performance, using the averaged aCC values among muscles (aCC average). We next assessed the level of variability (aCC variation, aCCvar) among muscle performance, using the maximal semi-dispersion (max-min/2) between the aCC of the three muscles. The selected muscles showed a rhythmic phasic activity during the ongoing task execution. The aCC enabled the estimation of the effect of DES on the rhythmicity/regularity of the phasic muscle contraction required by HMt execution for each muscle, while aCCvar enabled estimation of how much this regularity among muscles was affected by DES.

(2) The **Root Mean Square** (RMS) was estimated on the EMG activity according to the following formula:

$$RMS(x) = \sqrt{\frac{\sum_{i=1}^{N} {x_i}^2}{N}}$$

The RMS of each muscle during Effective and Ineffective Stimulation was normalized to the RMS activity of the corresponding muscle recorded at baseline according to the formula $RMS_{normalized} = RMS_{DES}/RMS_{baseline}$. We used the normalized averaged RMS among muscles to quantify the amount of motor units recruited during task execution (baseline and associated to LF-DES). This parameter allowed for estimation of the effect of DES on motor unit recruitment, irrespective of the rhythmicity of HMt execution (estimated by aCC), to disclose whether the effect of DES was excitatory or inhibitory with respect to the task-related muscle recruitment.

2.5.3. Detailed analysis of aCC

Correct execution of the HMt task was assessed by a regular EMG pattern. aCC average was used to evaluate LF-DES outcome, since it strictly reflected the regularity of the EMG pattern among muscles and thus the degree of patient behavioral performance. This analysis was chosen to distinguish, with respect to the baseline execution: (1) **Ineffective Sites**: no significant aCC average difference compared to the baseline execution; (2) **Effective Sites**: significant lower aCC average values compared to baseline. Significant lower aCC for each individual stimulated site was detected when the aCC average among muscles during LF-DES fell below 0.8. This criterion was chosen since in the present sample of patients a highly regular HMt execution during baseline showed an aCC average among muscles within the 0.8 – 1. Each aCC average value was associated to the corresponding aCCvar for each site to investigate the variability in the aCC among muscles. In the present study, each site (effective or ineffective) was represented by one stimulation trial.

2.5.4. Detailed analysis of RMS

Correct execution of the task, besides a regular EMG pattern, requires, for each muscle, an adequate amount of motor unit recruitment. RMS analysis was performed in order to study more specifically the effect of the DES on muscle recruitment during HMt execution. Significant difference in muscle recruitment for each effective site was detected when the normalized RMS average among muscles during LF-DES fell below 0.8 or above the 1.2. This criterion was chosen since in the present sample of patients a highly regular HMt execution during baseline showed a normalized RMS average among muscles within the 0.8–1.2 range.

2.6. Anatomo-functional reconstruction

For each patient, the reconstruction of the exact position of the Effective Sites and Ineffective Sites over the cortex was computed. During intraoperative mapping, the exposed craniotomy was video recorded, and the MRI coordinates of the sites were acquired using a neuronavigation system (Brainlab). To determine the exact position of the sites on the 3D MRI cortical surface of each patient the following procedure was adopted. The post-contrast T1-weighted sequence (TR/TE 2000/10 ms; FOV 230 mm; 176 slices; matrix, 400 × 512; SENSE factor 1.5) of each patient (the same loaded into the neuronavigation system during surgery) was used to perform the cortical surface extraction and surface volume registration computed with the FreeSurfer Software. Subsequently the results were loaded in a Matlab Tool Box, Brainstorm (Tadel et al. 2011), an accredited software freely available for download online under the GNU general public license (http://neuroimage.usc.edu/brainstorm). With the aid of Brainstorm, the exact site coordinates were marked on the patient's 3D MRI native space. Subsequently the MRI and site were co-registered to MNI space using unified segmentation implemented in SPM 12. The coordinates of each site of all patients were defined on the FSAverage template to create a 3D reconstruction of the left (stimulated) hemisphere (see Supplementary information Fig. 1). Due to anatomical variability among patients, particularly in this clinical setting, normalization steps may introduce some spatial inaccuracies. To avoid mismatching between native and MNI space, for each patient we checked the quality of the co-registration procedure (matching the native and MNI localization of the anterior and posterior commissures, median line and ventricles) and we visually inspected the location of the stimulated sites on the MNI template with respect to its localization in native space. All the sites reported in the present study matched with the original/native anatomical localization.

To investigate whether the Effective sites clustered in specific subsectors within the whole stimulated cortex, a modified in-house version of probability kernel density estimation (PDE analysis) implemented in MatLab was applied. The same method was applied in Fornia et al. (2020). Within this method the *smoothing* parameter or the *bandwidth*, select the window of observations, from the data sample that contributes to estimating the probability for a given sample. In the present study we choose as bandwidth for each coordinate (x,y,z) describing spatially each stimulated site the spread of current related to the LF-DES and the type of probe adopted (Ø 5mm). Since the stimulation points lay on a surface (the brain surface), the Euclidean distance does not represent the actual distance between stimulated sites. In order to calculate the distance between two points, the length of the shortest curve laying on the surface that connects them has been measured. Using a digital representation of the brain as a polygonal mesh surface, we can consider the mesh as a network of vertices connected by the edges. This way, a good approximation of the length of the shortest curve that connects two vertices can be the shortest path between the two edges that are closer to the sites: the denser the mesh in terms of vertices, the better the approximation. In the present study, the probability density estimation was based on the FSAverage template composed by 327684 vertices. The reconstructed probability density values are then calculated for a finite number of points onto the surface. To define the amount of points that covered the overall stimulated surface, a sampling parameter is used. The higher the value, the higher the number of points used, and showed for the estimation of the probability value. The results were plotted on the 3D FSAverage template (see Supplementary information Fig. 1) and their anatomical localization was estimated with probabilistic architectonic map available from the anatomy toolbox for SPM 12. In the present study 3 probability density estimations were performed:

(1) *Reliable sampling map*: Probability density estimation was performed for all the recorded stimulated sites. Regions with a sampling probability below the 15% were not considered due to a low sampling.

(2) *Eloquent map*. After distinction of effective and ineffective sites based on aCC analysis, probability density estimation for effective and ineffective sites was applied independently. Mathematical subtraction between probability maps was performed and visualized with the Computerized Anatomical Reconstruction Toolkit (CARET) in order to highlight the main "eloquent" sectors. Only sectors with a probability level above the 15%, and included within the reliable sampling map, were considered.
(3) *EMG-interference map*. Among effective sites, aCC analysis allowed to distinguish different EMG-interference patterns. The probability density estimation was performed for each pattern independently. Finally, the EMG-interference pattern probability maps were mathematically compared with CARET in order to highlight within the eloquent map which sectors were preferentially associated to a specific EMG-interference pattern. Only sectors included within the eloquent map were considered.
(4) *Muscle recruitment-suppression map*. Based on RMS analysis results among the EMG-interference patterns, different muscles recruitment-suppression effects were identity. The probability density estimation was performed on each type of muscle effect. The results were visualized with a probability threshold level above the 15%. Only sector within the eloquent map were considered.

3. Results

The analysis of EMG responses to LF-DES (EMG-interference pattern analysis) was performed on 280 stimulated sites (Fig. 1B) and their anatomical localization was identified (Fig. 1C). Postcentral gyrus (PCG) has been stimulated in 30 different patients, the posterior parietal cortex (PPC) in 26 different patients. Within PPC, superior parietal lobe (SPL) has been stimulated in 12 different patients, intraparietal cortex (IPC) in 14 different patients and inferior parietal lobe (IPL) in 21 different patients.

3.1. EMG-interference pattern analysis

With the EMG-interference pattern analysis, we evaluated the impact of LF-DES during HMt execution on selected intrinsic and extrinsic hand-muscles.

3.1.1. aCC analysis results

The analysis showed that LF-DES applied in 111 out of 280 stimulated sites in the parietal lobe significantly decreased the aCC of the investigated muscles during HMt execution (average stimulation sites for each patient n=8.2, SE±1.19; average effective sites for each patients n=3.2, SE±0.41, see also supplementary information ' 1). These sites were categorized as **effective sites**, while the sites failing to show significant changes on the aCC value were categorized as **ineffective sites**. Among the effective sites, two main EMG-interference patterns emerged (see Fig. 1B):

(1) *task-arrest patterns* (n = 51 sites recorded in 23 patients) referring to all the sites where stimulation evoked a complete abolishment of the EMG pattern required by HMt execution, occurring in all muscles, characterized by aCC average and variation = 0. From behavioral perspective, these patterns were associated to an abrupt arrest of the ongoing task execution.
(2) *task-clumsy patterns* (n = 60 sites recorded in 23 patients) referring to all the sites where stimulation evoked a partial disruption of the EMG pattern required by HMt execution and characterized by aCC average > 0 and < 0.8. Moreover, a negative correlation between aCC average and aCC var was found for the clumsy patterns (r=-0.48, p <.05) meaning that increasing value of aCC average was progressively associated to a more regular EMG pattern. See Fig. 1B. From behavioral perspective, these patterns were associated to a clear impairment of finger coordination and/or movement slowdown and loss of contact with the object.

3.1.2. RMS analysis results

The refined distribution of facilitation and inhibition among the muscles engaged during HMt execution was quantified by calculating the root mean square (RMS) of the EMG recorded in each selected muscle during HMt execution (both during and absence of LF-DES). Results showed the emergence, within the EMG-interference patterns, of three main effects on muscles:

(1) **Muscle suppression effect,** (N=79 sites recorded in 33 patients): normalized RMS average among muscles during LF-DES lower (< 0.8 normalized RMS average among muscles) compared to baseline. Among muscles at population level, one-way Anova showed that the RMS decrease was more pronounced in FDI and APB than in EDC (F=8.73, p=.000).
(2) **Muscle recruitment effect,** (N=10 sites recorded in 9 patients): normalized RMS average among muscles during LF-DES higher (> 1.2 normalized RMS average among muscles) compared to baseline. Among muscles at population level, the RMS increase was more pronounced in FDI and EDC than APB (F=4.76, p=.014).
(3) **Muscle mixed effect:** in N=22 effective sites (recorded in 16 patients), despite a significant decrease in aCC average value, the normalized RMS average among muscles during LF-DES fell within a range similar to baseline (0.8-1.2). Among muscles at population level, no significant differences emerged (F=2.75, p=.070).

When matching results obtained with aCC and RMS analysis (see Fig. 1B), it emerged that: (1) among **muscle suppression sites**, n=35 were task-arrest patterns while n=44 task-clumsy patterns; (2) among **muscle recruitment sites**, all (n = 10) were task-arrest patterns. The remaining **muscle mixed effects,** were mostly clumsy pattern (n = 16 out of 22).

3.2. Anatomo-functional reconstruction

(1) *Reliable sampling map*. A reliable stimulation sampling covered the majority of the parietal sectors, including the inferior parietal lobe, the superior parietal lobe (excluding area 5L) and the intraparietal sulcus (Fig. 1C).
(2) *Eloquent map*. The most "eloquent" sectors fell in the PCG fingers representation (BA1/2, primary somatosensory cortex) and within PPC at the junction between intraparietal and postcentral sulcus, involving areas around the anterior intraparietal cortices (aIPC, mainly hIP2 and PFt). Both sectors were included within the reliable sampling map. Marginally, some effective sites were also found in area 5L and on the convexity of the anterior supramargynal gyrus (aSMG/BA40). However, area 5L fell outside the reliable sampling map, while aSMG (although within the reliable sampling map) fell outside the eloquent map (Fig. 1D).
(3) *EMG-interference map*. aCC analysis revealed the occurrence of two different EMG-interference patterns: task-arrest and clumsy pattern. From their respective probability maps emerged a preferential (although not exclusive) distribution (Fig. 1E), becoming clearer after subtraction of the two maps. We identified 3 main clusters localized within the eloquent maps (Fig. 1F).
   - *PCG clusters*. Cluster 1 hosted prevalently task-arrest patterns falling in the medial hand-finger somatosensory representation, while cluster 2, more lateral with respect to cluster 1, hosted a prevalence of task-clumsy patterns.
   - *PPC cluster*. Located within the junction between intraparietal and postcentral sulcus (aIPC), this cluster hosted with higher probability task-arrest patterns. Although within PPC task-clumsy pattern were not absent, their occurred preferentially within aSMG (Fig. 1E), a sector, as discussed before, falling outside the eloquent map, preventing, at present, reliable conclusion.

(4) *Muscle suppression-recruitment map*. Probability density maps for muscles suppression, recruitment and mixed effects were performed and visualized with a threshold above 15% of probability and overlapped with the eloquent map borders (Fig. 2A–C).

- *Muscle suppression map*. Previous RMS analysis showed that muscle suppression was the most common effect in both PCG and PPC clusters and, coherently, its probability map covered both sectors (Fig. 2A). However, statistical analysis showed that stimulation of PPC was generally associated to higher magnitude of muscles suppression than PCG (F=14.173, p=.000). Interaction between task and area showed that this effect was mainly associated to task-arrest, rather than task-clumsy (F=5.318, p=.023) (Fig. 2A).
- *Muscle recruitment and mixed map*. Within PCG clustered other muscle effects, absent within PPC. The posterior sector of the PCG cluster 1 showed higher probability for muscle recruitment associated to task-arrest pattern, while PCG cluster 2 showed higher probability for muscle mixed effects associated to task-clumsy pattern (respectively Fig. 2B,C).

4. Discussion

The role of parietal cortex in control of hand-object manipulation is not questionable. However, this topic has never been investigated with a focal and direct electrophysiological approach in humans. To this aim, in the present study, we investigated the impact of LF-DES delivered during neurosurgical procedure over the parietal lobe on the activity of extrinsic and intrinsic hand muscles during a haptically driven hand-object interaction task in thirty-four human brain tumor patients. Should the parietal lobe be involved in object manipulation and its related hand-muscle control, LF-DES would disrupt HMt ongoing execution (and the related hand-muscles activity) only when applied on parietal sectors functionally involved in task execution by shaping the motor output to muscles and/or the flow of sensorimotor integration. A lack of effect on HMt execution and its hand-muscle activity would reflect the stimulation of a parietal sector not primarily involved neither in shaping the motor output to muscles nor in the sensorimotor integration required by task.

4.1. Functional aspects associated to the different EMG-interference patterns

Two main EMG-interference patterns emerged: the **task-arrest pattern** characterized by a complete impairment of the phasic and time-dependent muscle contraction associated with a sudden interruption of task execution; the **task-clumsy pattern** associated to a partial impairment with a clear decrease of finger coordination and/or movement slowdown and loss of contact with the object. During clumsy patterns, a residual irregular muscle phasic activity was thus still present with respect to arrest pattern (Fig. 1B). The complementary RMS analysis revealed that both patterns were associated mainly to a general muscle suppression (72% of the cases, see single trial examples from representative patients in Fig. 2A1–5). Rarely, the task-arrest pattern was also associated to a muscle recruitment (9% of the case, see single trial example in Fig. 2B1), although not systematically detected in all muscles (see single trial example in Fig. 2B2: EDC and FDI recruitment much higher than APB). Challenging to interpret are the 19% of the sites categorized as muscle mixed effects, prevalently task-clumsy, possibly due to milder effects of recruitment and/or coexistence of both suppression-recruitment effects (see single trial example in Fig. 2C). Hypothetically, the different EMG-interference patterns evoked by LF-DES might reflect different functional aspects. In particular, that the **task-arrest pattern** might reflect the DES-related interference of a parietal substrate closely implicated in shaping motor output to muscles. Differently, **the task-clumsy pattern**, being characterized by an impairment of the quality of movements rather than by a complete task interruption, might reflect a parietal substrate that acts remotely on motor output. Indeed, clumsy movements might be symptom of an impairment at the level of sensorimotor integration, affecting smoothness and coordination of fingers movements.

4.2. Localization of Effective sites within human PCG and PPC

The preferential occurrence of EMG-interference patterns in specific sectors (see eloquent map) deserved a discussion. Within PPC, effective sites were found mainly within aIPC, at the junction between intraparietal and postcentral sulcus (Fig. 1C). This sector, largely corresponding to phAIP functional region (Orban, 2016) suggested to be part of the human homologue of the monkey AIP, is a region crucially involved in sensorimotor integration during grasping and object-manipulation. In this regard, it has been proposed that human phAIP, and the adjacent dorsal sector in the anterior intraparietal sulcus (DIPSA), may correspond to the anterior motor-dominant and posterior visuo-dominant part of monkey AIP, respectively (Orban, 2016). Supporting this hypothesis, in the present study LF-DES impaired muscle performance mainly when applied within phAIP (not in DIPSA, see Fig. 1D). This result highlights the “motor attitude” or, given the strong hand somatosensory information reaching the most anterior part of phAIP (Avanzini et al., 2016), the “somatomotor attitude” of this sector respect to the dorsal one. The specific hand manipulation task (HMt) chosen in the present study, relying exclusively on somatosensory feedback, further supports this hypothesis. Indeed, HMt was adopted in order to avoid possible interference due to visual or visuo-motor impairment evoked by DES during performance, focusing mainly on the motor/somatomotor features of the parietal lobe. The human AIP represents a central hub for moving across different level of action representation, from pragmatic action representation (concrete action specification) to abstract action representation (Turella et al., 2020, Monaco et al., 2020; Gallivan et al., 2013a). Our results lead to hypothesize that within the pragmatic aspects, a role in shaping hand-motor output to muscles during dexterous task might be included. The convergence of these features within this sector might suggests its pivotal role in flexibly organizing low-level features of action, such as kinetic and kinematic aspects.

Comparing our eloquent map with fMRI activations in human parietal areas during grasping execution, it emerges that although our eloquent sites are located within parietal sector identified by fMRI, they lay on a narrower surface compare to that showed in neuroimaging studies (Errante et al., 2021; Gallivan et al., 2011; Gallivan et al., 2013a). This discrepancy might be explained by different factors. In particular, the nature of the present intraoperative task and its differences with grasping tasks employed during fMRI experiment is relevant. (1) The HMt was not a discreet movement, it was performed continuously and with a self-paced rhythm; (2) The HMt was haptically driven, no visual information was required. These features avoided the visuo-motor integration and the eye-hand coordination, possibly decreasing the load on parietal regions implicated in those aspects. 3) Finally, the probability map derived from DES and statistical map derived by fMRI are generated from different substrates. DES reveals a causal link between the region stimulated and the observed effect. In the fMRI, this link is correlational and indirectly generated by neuronal activity. However, despite these aspects, we have to evidence that the present eloquent map seems in agreement with fMRI local maxima showed by Konen et al. (2013), specifically investigating the portion of posterior parietal cortex coding grasping actions.

Within PCG, the effective sites were identified in a middle-lateral portion of BA1/2. LF-DES on PCG during HMt (both effective and ineffective stimulations) rarely elicited somatic sensations, despite overtly perceived inability to execute the task during effective stimulations (Fornia et al., 2020b). Somatic sensations evoked by LF-DES at rest were not systematically investigated in the present study, preventing us to correlate somatic sensation with task-related impairment. However, within the PCG the effective sites and their related probability map are

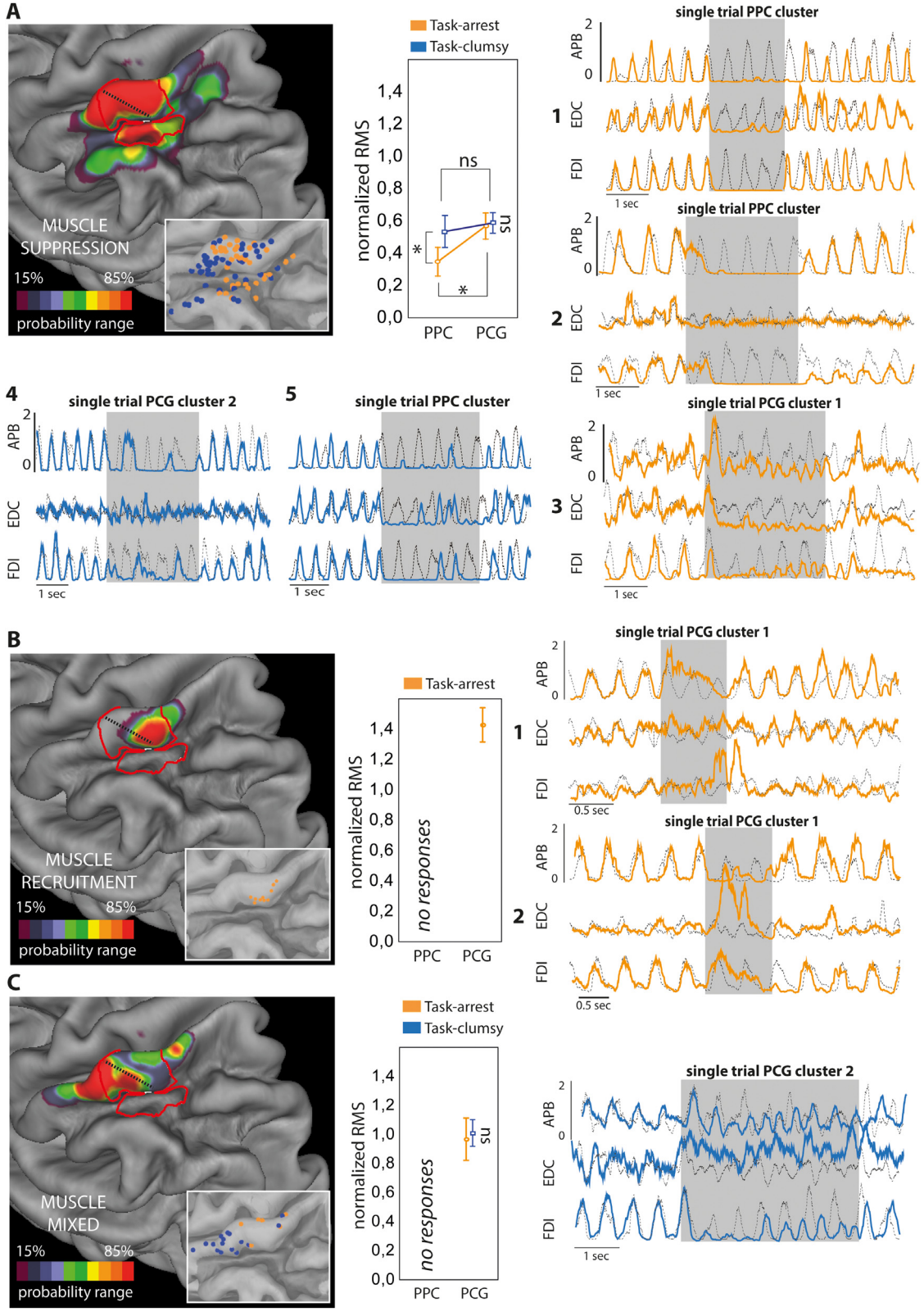

Fig. 2. (A) Probability density estimation for the muscle suppression effects overlapped with border of the eloquent map (in red) was associated with the related statistical analysis and examples of single trial EMG-interference patterns associated to muscles suppression from representative patients: 1-2 single trails of task-arrest observed within aPPC cluster; 3 single trial task-arrest observed within PCG cluster 1; 4-5 single trial task-clumsy observed, respectively within PCG cluster 2 and aSMG (not within eloquent map). **(B) Probability density estimation for the muscle recruitment effects** overlapped with border of the eloquent map was associated with the related statistical analysis and examples of single trials EMG-interference patterns associated to muscles recruitment from representative patients: 1-2 single trials of task-arrest observed within caudal PCG cluster. 1. **(C) Probability density estimation for the muscle mixed effects** overlapped with border of the eloquent map was associated with the related statistical analysis and an example of single trial EMG-interference patterns associated to muscles mixed from representative patients within PCG cluster 2. In A-B-C the dashed black line on PCG divided cluster 1 from cluster 2. (For interpretation of the references to color in this figure legend, the reader is referred to the web version of this article).

located where DES evoked fingers somatic sensations at rest according to Roux et al. (Roux et al. 2018). This aspect suggest that at population level most of the present effective sites in PCG belonged to the fingers representation.

Concerning the absence of somatic sensations reported during HMt execution, this observation seems in line with evidence that movement-related cortical activity physiologically inhibits the somatosensory computation at neural level (Seki et al. 2012; Starr et al. 1985) and its perception (Chapman et al. 1987; Angel et al. 1982) during voluntary movements. Accordingly, we exclude that the EMG-interference patterns evoked within PCG were indirectly triggered by an evoked "discomfort" somesthetic sensations. Rather, a functional interpretation pointing to a role of PCG in shaping and controlling the voluntary motor output resonate better with some fMRI studies. It has been shown that activation of fingers representation in PCG correlates with several motor aspects during voluntary movement, including encoding of hand muscles synergies associated to specific hand posture (Leo et al., 2016), activity in motor-premotor cortex and motor units recruitment during hand motor task (Cui et al. 2014). Moreover, following a precentral lesion, PCG functional reorganization seems correlated to a partial recovery of the hand-arm movements with their associated muscles synergies (Godlove et al. 2016). Finally, a recent fMRI study has shown that specific subsectors of PCG during planning of manipulative actions are modulated in parallel with activity in primary motor cortex, suggesting the crucial role of PCG areas in motor control, possibly contributing during movement preparation at a sensory prediction of incoming action (Gale et al. 2021). Evidences of the role of SI in motor control comes also from non-human primates studies, showing that specific SI sector encode differently passive from active arm-hand movements (Chowdhury et al. 2020) and its activity reflects both primary motor cortex activation and sensory feedback at different delays respect to the planning and execution phase (Umeda et al., 2019).

4.3. Anatomo-functional organization of EMG-interference patterns

According to the functional hypothesis suggested for the EMG-interference patterns, within PCG the medial BA1/2 and aIPC, preferentially associated to task-arrest pattern (PCG cluster 1 and aIPC), might be part of neuronal substrates closely implicated in the shaping of the voluntary motor output to muscles. Differently, the lateral BA1/2, preferentially associated to task clumsy pattern (PCG cluster 2), might act more indirectly respect to the motor output. In this light clumsy pattern might reflect a problem in the sensorimotor integration required by HMt execution (Fig. 1E,F).

The medio-lateral organization of the EMG-interference patterns within primary somatosensory fingers representation seems to reflect a functional organization suggested also by tractography results showing distinct dorso-lateral U-shaped tracts connecting PCG with precentral hand-knob region (Catani et al. 2012; Pron et al., 2021). Moreover, PCG fingers representation host connections with different posterior parietal areas (Catani et al., 2017). The medial PCG (including PCG cluster 1) connects with the angular gyrus and SPL, while the lateral portion (including PCG cluster 2) connects with the anterior supramargynal gyrus (aSMG). However, stimulation within SPL and aSMG rarely interfered with hand-muscle control during task (see single trial example in Fig. 2A5 and Video 1); being both regions outside from the eloquent map, preventing at this moment further discussions.

Interestingly, significant differences emerged within the eloquent map between PCG clusters and aIPC. Muscle recruitment (see Video 2) and mixed effects (see Video 3), although numerically lower respect to suppression, were recorded exclusively in PCG. Moreover, statistical analysis revealed that, although muscle suppression was recorded in both PCG and aIPC, in the latter a higher magnitude of DES-related suppression occurred, especially when associated to task-arrest (Fig. 2A). This seems coherent with the qualitative observation that in aIPC the suppression pattern in most of the cases resembled the hypotonic-like effect (see single trial example Fig. 2A1-2 see Video 4 and 5) observed in ventral premotor cortex (Fornia et al., 2020). Differently, in PCG the suppression pattern was associated often to a residual muscle activity (see Video 6 and 7) or clonic-like twitches observable at behavioral level (see single trial example Fig. 2A3 and Video 8) during all the stimulation period. These observations suggest that, although LF-DES suppressed in both PCG and aIPC the muscle activity required by task execution, the features of the suppression were significantly different in the two parietal sectors. Summarizing, in PCG the LF-DES during task evoked variable levels of muscles recruitment, ranging from the subtle muscle activity during the suppression effects to the more evident muscle recruitment effects associated to an overt involuntary hand movements. Differently, within aIPC, the muscle activity during the suppression effect was comparable to a rest condition. This result suggests that different parietal sectors might synergically shape the motor output to hand-muscle by balancing inhibitory and facilitatory inputs. Hodological studies in monkeys suggest that these inputs might be potentially organized via direct (corticospinal) or indirect (parietal-premotor) connections with spinal circuits. Based on parieto-frontal control of hand-muscles, the present parietal effects might reflect curtailment of downstream processing in the frontal sites. This is plausible in the light of the similar results observed in the premotor areas with the same methodology (Fornia et al., 2020). In this frame, we might also speculate that task-arrest related sectors (PCG cluster 1 and aIPC cluster), due to a massive effect on muscle recruitment, might exert their influence on motor output via direct connections with primary motor cortex and/or corticospinal tract directly modulating the excitability of spinal circuits. Differently, task-clumsy related sector (mainly PCG cluster 2, but reported also in aIPC and aSMG) patterns might be evoked by DES-interference on parietal-premotor loops, affecting their functional role in sensorimotor integration for hand action. LF-DES might affect the inflow of information required by premotor area for selecting the correct hand-motor schema during the different phases of the ongoing HMt execution. However, dedicated studies are mandatory to address the anatomical substrates behind these parietal effects evoked by DES. Possible insight about the pathways involved by posterior parietal cortex to modulate the motor output come from a recent intraoperative study in asleep brain tumor patients. Cattaneo and coworkers (Cattaneo et al., 2020) reported inhibitory effects on motor output after short delay conditioning stimulus delivered across the junction between intraparietal and post-central sulcus, a region very likely corresponding at convexity level to the present aIPC cluster. The author suggested that the effects obtained at short-delay might underline the presence of direct connection between the aPPC and precentral cortex capable of modulating its output to hand-muscles.

Finally, parietal lesion in both human and non-human primate often evoke transient hypotonia, weakness of the contralateral extremities (Fleming and Crosby, 1955; Mountcastle et al., 1975), praxis (Goldenberg, 2009) and fingers coordination deficits (Janssen et al., 2015, Binkofski et al., 1998). These symptoms resemble from behavioral point of view the effects evoked by parietal LF-DES, associated to muscle suppression, hypotonic-like behaviors and clumsy-hand. Mountcastle and coworkers based on properties of parietal hand-manipulation neurons suggested that these symptoms were the consequence of the impairment of the *command apparatus* embedded in the parietal lobe. In line with Mountcastle hypothesis, the present results obtained with a direct electrophysiological approach in humans strongly corroborate the crucial role of the parietal lobe as command apparatus for hand action.

4.4. Limitations of the study

The specific limitations of the study deserve a discussion. (A) One of the main limitations of DES approach in humans is that its neurophysiological substrate is not yet fully clarified (Borchers et al. 2011),

challenging data interpretation and therefore allowing us only to suggest further hypotheses rather than conclusions. Irrespectively to the neurophysiological mechanism of DES, the strong causality between the stimulation, the concomitant behavioral outcome, and the post-surgical clinical outcome of patients leads DES to be considered the "gold standard for brain mapping" in systems neuroscience (Mandonnet et al., 2010), including motor (Fornia et al., 2020b; Viganò et al. 2021; Viganò et al. 2019) and cognitive functions (Puglisi et al., 2019). (B) The localization of the tumor within the white matter of parietal lobe could affect the reliability of the results. However, this limitation was avoided as much as possible by integrating data coming from different patients: (1) patients with brain tumor not infiltrating the parietal lobe, but requiring its partial exposure and its stimulation for clinical reasons; (2) patients with parietal tumors occupying a small white matter volume. Moreover, probabilistic population analysis coming from a large cohort of patients should also contributes to partially compensate for such aspects. (C) The strict comparison of the DES-related results with standard non-invasive stimulation techniques is challenging, since the latter are behavioral state-dependent. In fact, due to clinical constraints, LF-DES was delivered randomly during HMt execution, rather than locked to specific task-phases. Although we cannot exclude that stimulation of the same site at different task-phases might evoke different muscles effects, the emergence of EMG-interference clusters suggested that results should not be relevantly influenced by this aspect. (D) Since the effective sites reported were not tested, for clinical constraints, for other effectors (e.g oro-facial movements) we cannot exclude that these sites were also involved in controlling muscles driving other effectors. Notably, the same sites failed to interfere with speech motor production, supporting a segregation based on effector. However, the possible remote effects evoked by DES (Borchers et al., 2011) might affect this aspect. In this regard, spatial correspondence between eloquent map and others studies investigating grasping/object manipulation in parietal lobe (Konen et al., 2013) and somatosensory homunculus along the PCG (Roux et al., 2018) seems indirectly confirm that the eloquent map belong mainly to parietal hand/fingers-related areas. (E) Finally, all the stimulated sites were selected based on clinical needs and not based on research purposes. This prevents a homogeneous selection in all patients of specific target region a priori, as occurs in standard non-invasive stimulation protocols. This aspect inevitably causes some patients to weight more of others in terms of information (e.g. stimulation sites). However, merging information from a huge cohort of patients is helpful in reducing the impact of this unavoidable aspect.

5. Conclusion

Despite several studies in human provide evidence with non-invasive techniques about the involvement of parietal lobe in object manipulation and grasping action, this topic has never been investigated with a direct (invasive) and focal electrophysiological method. We approached this topic by using LF-DES in awake patients performing a dedicated HMt and simultaneously recording activity from hand-muscles. LF-DES affects hand-muscle control during task execution when delivered on the parietal lobe and specifically on sites corresponding to hand/fingers region within the PCG and in the anterior sector of IPS. The specific task employed in the present intraoperative study, requiring a high dexterity due to hand-object interaction, allowed to revealing the occurrence of different DES- related EMG-interference patterns segregated in different anterior and posterior parietal sectors. It could be suggested that these patterns might reflect different functional aspects associated to the involvement of the parietal cortex in shaping primary motor output to muscles and sensorimotor integration.

Acknowledgments

This work has been supported by "Regione Lombardia" under the Eloquentstim Project (PorFesr, 2014–2020) and by funds 18482 from AIRC (Associazione Italiana Ricerca sul Cancro) to LB.

Supplementary materials

Supplementary material associated with this article can be found, in the online version, at doi:10.1016/j.neuroimage.2021.118839.

References

Angel, R.W., Malenka, R.C., 1982. Velocity-dependent suppression of cutaneous sensitivity during movement. Exp. Neurol. 77 (2), 266–274. doi:10.1016/0014-4886(82)90244-8.

Avanzini, P., Abdollahi, R.O., Sartori, I., Caruana, F., Pelliccia, V., Casaceli, G., Mai, R., Lo Russo, G., Rizzolatti, G., Orban, G.A., 2016. Four-dimensional maps of the human somatosensory system. Proc. Natl. Acad. Sci. U. S. A. 113 (13), E1936–E1943. doi:10.1073/pnas.1601889113.

Bello, L., Riva, M., Fava, E., Ferpozzi, V., Castellano, A., Raneri, F., Pessina, F., Bizzi, A., Falini, A., Cerri, G., 2014. Tailoring neurophysiological strategies with clinical context enhances resection and safety and expands indications in gliomas involving motor pathways. Neuro Oncol. 16 (8), 1110–1128. doi:10.1093/neuonc/not327.

Binkofski, F., Dohle, C., Posse, S., Stephan, K.M., Hefter, H., Seitz, R.J., Freund, H.J., 1998. Human anterior intraparietal area subserves prehension: a combined lesion and functional MRI activation study. Neurology 50 (5), 1253–1259. doi:10.1212/wnl.50.5.1253.

Borchers, S., Himmelbach, M., Logothetis, N., Karnath, H.O., 2011. Direct electrical stimulation of human cortex - the gold standard for mapping brain functions? Nat. Rev. Neurosci. 13 (1), 63–70. doi:10.1038/nrn3140.

Borra, E., Gerbella, M., Rozzi, S., Luppino, G., 2017. The macaque lateral grasping network: A neural substrate for generating purposeful hand actions. Neurosci. Biobehav. Rev. 75, 65–90. doi:10.1016/j.neubiorev.2017.01.017.

Catani, M., Dell'acqua, F., Vergani, F., Malik, F., Hodge, H., Roy, P., Valabregue, R., Thiebaut de Schotten, M., 2012. Short frontal lobe connections of the human brain. Cortex 48 (2), 273–291. doi:10.1016/j.cortex.2011.12.001.

Catani, M., Robertsson, N., Beyh, A., Huynh, V., de Santiago Requejo, F., Howells, H., Barrett, R., Aiello, M., Cavaliere, C., Dyrby, T.B., Krug, K., Ptito, M., D'Arceuil, H., Forkel, S.J., Dell'Acqua, F., 2017. Short parietal lobe connections of the human and monkey brain. Cortex 97, 339–357. doi:10.1016/j.cortex.2017.10.022.

Cattaneo, L., Giampiccolo, D., Meneghelli, P., Tramontano, V., Sala, F., 2020. Cortico-cortical connectivity between the superior and inferior parietal lobules and the motor cortex assessed by intraoperative dual cortical stimulation. Brain Stimulat. 13 (3), 819–831. doi:10.1016/j.brs.2020.02.023.

Cerri, G., Shimazu, H., Maier, M.A., Lemon, R.N., 2003. Facilitation from ventral premotor cortex of primary motor cortex outputs to macaque hand muscles. J. Neurophysiol. 90 (2), 832–842. doi:10.1152/jn.01026.2002.

Chapman, C.E., Bushnell, M.C., Miron, D., Duncan, G.H., Lund, J.P., 1987. Sensory perception during movement in man. Exp. Brain Res. 68 (3), 516–524. doi:10.1007/BF00249795.

Chowdhury, R.H., Glaser, J.I., Miller, L.E, 2020. Area 2 of primary somatosensory cortex encodes kinematics of the whole arm. Elife 9, e48198. doi:10.7554/eLife.48198.

Conti Nibali, M., Leonetti, A., Puglisi, G., Rossi, M., Sciortino, T., Gay, L.G., Arcidiacono, U.A., Howells, H., Viganò, L., Zito, P.C., Riva, M., Bello, L., 2020. Preserving visual functions during gliomas resection: feasibility and efficacy of a novel intraoperative task for awake brain surgery. Front. Oncol. 10, 1485. doi:10.3389/fonc.2020.01485.

Côté, S.L., Hamadjida, A., Quessy, S., Dancause, N., 2017. Contrasting modulatory effects from the dorsal and ventral premotor cortex on primary motor cortex outputs. J. Neurosci. 37 (24), 5960–5973. doi:10.1523/JNEUROSCI.0462-17.2017.

Cui, F., Arnstein, D., Thomas, R.M., Maurits, N.M., Keysers, C., Gazzola, V., 2014. Functional magnetic resonance imaging connectivity analyses reveal efference-copy to primary somatosensory area, BA2. PloS one. 9 (1), e84367. doi:10.1371/journal.pone.0084367.

Bäumer, T., Schippling, S., Kroeger, J., Zittel, S., Koch, G., Thomalla, G., Rothwell, J.C., Siebner, H.R., Orth, M., Münchau, A., 2009. Inhibitory and facilitatory connectivity from ventral premotor to primary motor cortex in healthy humans at rest - a bifocal TMS study. Clin. Neurophysiol. 120 (9), 1724–1731. doi:10.1016/j.clinph.2009.07.035.

Davare, M., Montague, K., Olivier, E., Rothwell, J.C., Lemon, R.N, 2009. Ventral premotor to primary motor cortical interactions during object-driven grasp in humans. Cortex 45 (9), 1050–1057. doi:10.1016/j.cortex.2009.02.011.

Davare, M., Andres, M., Clerget, E., Thonnard, J.L., Olivier, E., 2007. Temporal dissociation between hand shaping and grip force scaling in the anterior intraparietal area. J. Neurosci. 27 (15), 3974–3980. doi:10.1523/JNEUROSCI.0426-07.2007.

Davare, M., Lemon, R., Olivier, E., 2008. Selective modulation of interactions between ventral premotor cortex and primary motor cortex during precision grasping in humans. J. Physiol. 586 (11), 2735–2742. doi:10.1113/jphysiol.2008.152603.

Desmurget, M., Richard, N., Beuriat, P.A., Szathmari, A., Mottolese, C., Duhamel, J.R., Sirigu, A., 2018. Selective inhibition of volitional hand movements after stimulation of the dorsoposterior parietal cortex in humans. Curr. Bio. 28 (20), 3303–3309. doi:10.1016/j.cub.2018.08.027, e3.

Desmurget, M., Sirigu, A., 2015. Revealing humans' sensorimotor functions with electrical cortical stimulation. Philos. Trans. R. Soc. Lond. B Biol. Sci. 370 (1677), 20140207. doi:10.1098/rstb.2014.0207.

Errante, A., Ziccarelli, S., Mingolla, G., Fogassi, L., 2021. Grasping and manipulation: neural bases and anatomical circuitry in humans. Neuroscience 458, 203–212. doi:10.1016/j.neuroscience.2021.01.028.

FLEMING, J.F., CROSBY, E.C., 1955. The parietal lobe as an additional motor area; the motor effects of electrical stimulation and ablation of cortical areas 5 and 7 in monkeys. J. Comp. Neurol. 103 (3), 485–512. doi:10.1002/cne.901030306.
Fornia, L., Ferpozzi, V., Montagna, M., Rossi, M., Riva, M., Pessina, F., Martinelli Boneschi, F., Borroni, P., Lemon, R.N., Bello, L., Cerri, G., 2018. Functional characterization of the left ventrolateral premotor cortex in humans: a direct electrophysiological approach. Cereb. Cortex. 28 (1), 167–183. doi:10.1093/cercor/bhw365.
Fornia, L., Puglisi, G., Leonetti, A., Bello, L., Berti, A., Cerri, G., Garbarini, F., 2020. Direct electrical stimulation of the premotor cortex shuts down awareness of voluntary actions. Nat. Comm. 11 (1), 705. doi:10.1038/s41467-020-14517-4.
Fornia, L., Rossi, M., Rabuffetti, M., Leonetti, A., Puglisi, G., Viganò, L., Simone, L., Howells, H., Bellacicca, A., Bello, L., Cerri, G., 2020. Direct electrical stimulation of premotor areas: different effects on hand muscle activity during object manipulation. Cereb. Cortex. 30 (1), 391–405. doi:10.1093/cercor/bhz139.
Gale, D.J., Flanagan, J.R, Gallivan, J.P., 2021. Human somatosensory cortex is modulated during motor planning. J. Neurosci. 41 (27), 5909–5922. doi:10.1523/JNEUROSCI.0342-21.2021.
Gallivan, J.P., McLean, D.A., Flanagan, J.R., Culham, J.C., 2013. Where one hand meets the other: limb-specific and action-dependent movement plans decoded from preparatory signals in single human frontoparietal brain areas. J. Neurosci. 33 (5), 1991–2008. doi:10.1523/JNEUROSCI.0541-12.2013.
Gallivan, J.P., Culham, J.C, 2015. Neural coding within human brain areas involved in actions. Curr. Opin. Neurobiol. 33, 141–149. doi:10.1016/j.conb.2015.03.012.
Gharbawie, O.A., Stepniewska, I., Qi, H., Kaas, J.H., 2011. Multiple parietal-frontal pathways mediate grasping in macaque monkeys. J. Neurosci. 31 (32), 11660–11677. doi:10.1523/JNEUROSCI.1777-11.2011.
Godlove, J., Gulati, T., Dichter, B., Chang, E., Ganguly, K., 2016. Muscle synergies after stroke are correlated with perilesional high gamma. Ann. Clin. Transl. Neurol. 3 (12), 956–961. doi:10.1002/acn3.368.
Goldenberg, G., 2009. Apraxia and the parietal lobes. Neuropsychologia 47 (6), 1449–1459. doi:10.1016/j.neuropsychologia.2008.07.014.
Innocenti, G.M., Caminiti, R., Rouiller, E.M., Knott, G., Dyrby, T.B., Descoteaux, M., Thiran, J.P., 2019. Diversity of cortico-descending projections: histological and diffusion MRI characterization in the monkey. Cereb. Cortex 29 (2), 788–801. doi:10.1093/cercor/bhx363.
Janssen, P., Scherberger, H., 2015. Visual guidance in control of grasping. Annu. Rev. Neurosci. 38, 69–86. doi:10.1146/annurev-neuro-071714-034028.
Kaneko, T., Caria, M.A., Asanuma, H., 1994. Information processing within the motor cortex. I. Responses of morphologically identified motor cortical cells to stimulation of the somatosensory cortex. J. Comp. Neurol. 345 (2), 161–171. doi:10.1002/cne.903450202.
Koch, G., Rothwell, J.C, 2009. TMS investigations into the task-dependent functional interplay between human posterior parietal and motor cortex. Behav. Brain Res. 202 (2), 147–152. doi:10.1016/j.bbr.2009.03.023.
Koch, G., Fernandez Del Olmo, M., Cheeran, B., Ruge, D., Schippling, S., Caltagirone, C., Rothwell, J.C., 2007. Focal stimulation of the posterior parietal cortex increases the excitability of the ipsilateral motor cortex. J. Neurosci. doi:10.1523/JNEUROSCI.0598-07.2007.
Leo, A., Handjaras, G., Bianchi, M., Marino, H., Gabiccini, M., Guidi, A., Scilingo, E.P., Pietrini, P., Bicchi, A., Santello, M., Ricciardi, E., 2016. A synergy-based hand control is encoded in human motor cortical areas. eLife. 5, e13420. doi:10.7554/eLife.13420.
Monaco, S., Malfatti, G., Culham, J.C., Cattaneo, L., Turella, L., 2020. Decoding motor imagery and action planning in the early visual cortex: Overlapping but distinct neural mechanisms. Neuroimage 218, 116981. doi:10.1016/j.neuroimage.2020.116981.
Mountcastle, V.B., Lynch, J.C., Georgopoulos, A., Sakata, H., Acuna, C., 1975. Posterior parietal association cortex of the monkey: command functions for operations within extrapersonal space. J. Neurophysiol. 38 (4), 871–908. doi:10.1152/jn.1975.38.4.871.
Nelissen, K., Vanduffel, W., 2011. Grasping-related functional magnetic resonance imaging brain responses in the macaque monkey. J. Neurosci. 31 (22), 8220–8229. doi:10.1523/JNEUROSCI.0623-11.2011.
Nelson-Wong, E., Howarth, S., Winter, D.A., Callaghan, J.P., 2009. Application of autocorrelation and cross-correlation analyses in human movement and rehabilitation research. Orthop. Sports Phys. Ther. 39 (4), 287–295. doi:10.2519/jospt.2009.2969.
Nudo, R.J., Masterton, R.B., 1990. Descending pathways to the spinal cord, IV: Some factors related to the amount of cortex devoted to the corticospinal tract. J. Comp. Neurol. 296 (4), 584–597. doi:10.1002/cne.902960406.
Orban, G.A., 2016. Functional definitions of parietal areas in human and non-human primates. Proc. Biol. Sci. 283 (1828), 20160118. doi:10.1098/rspb.2016.0118.
Parikh, P.J., Fine, J.M., Santello, M., 2020. Dexterous object manipulation requires context-dependent sensorimotor cortical interactions in humans. Cereb. Cortex 30 (5), 3087–3101. doi:10.1093/cercor/bhz296.
Prabhu, G., Shimazu, H., Cerri, G., Brochier, T., Spinks, R.L., Maier, M.A., Lemon, R.N., 2009. Modulation of primary motor cortex outputs from ventral premotor cortex during visually guided grasp in the macaque monkey. J. Physiol. 587 (Pt 5), 1057–1069. doi:10.1113/jphysiol.2008.165571.
Pron, A., Deruelle, C., Coulon, O., 2021. U-shape short-range extrinsic connectivity organisation around the human central sulcus. Brain Struct. Funct. 226 (1), 179–193. doi:10.1007/s00429-020-02177-5.
Puglisi, G, Howells, H, Sciortino, T, Leonetti, A, Rossi, M, Conti Nibali, M, Gabriel Gay, L, Fornia, L, Bellacicca, A, Viganò, L, Simone, L, Catani, M, Cerri, G, Bello, L., 2019. Frontal pathways in cognitive control: direct evidence from intraoperative stimulation and diffusion tractography. Brain 1 (8), 2451–2465. doi:10.1093/brain/awz178, 142.
Rathelot, J.A., Dum, R.P., Strick, P.L., 2017. Posterior parietal cortex contains a command apparatus for hand movements. Proc. Natl. Acad. Sci. U. S. A. 114 (16), 4255–4260. doi:10.1073/pnas.1608132114.
Rech, F., Herbet, G., Gaudeau, Y., Mézières, S., Moureau, J.M., Moritz-Gasser, S., Duffau, H., 2019. A probabilistic map of negative motor areas of the upper limb and face: a brain stimulation study. Brain 142 (4), 952–965. doi:10.1093/brain/awz021.
Rossi, M., Fornia, L., Puglisi, G., Leonetti, A., Zuccon, G., Fava, E., Milani, D., Casarotti, A., Riva, M., Pessina, F., Cerri, G., Bello, L., 2018. Assessment of the praxis circuit in glioma surgery to reduce the incidence of postoperative and long-term apraxia: a new intraoperative test. J. Neurosurg. 130 (1), 17–27. doi:10.3171/2017.7.JNS17357.
Rossi, M., Conti Nibali, M., Viganò, L., Puglisi, G., Howells, H., Gay, L., Sciortino, T., Leonetti, A., Riva, M., Fornia, L., Cerri, G., Bello, L., 2019. Resection of tumors within the primary motor cortex using high-frequency stimulation: oncological and functional efficiency of this versatile approach based on clinical conditions. J. Neurosurg. doi:10.3171/2019.5.JNS19453.
Rossi, M., Viganò, L., Puglisi, G., Conti Nibali, M., Leonetti, A., Gay, L., Sciortino, T., Fornia, L., Callipo, V., Lamperti, M., Riva, M., Cerri, G., Bello, L., 2021a. Targeting primary motor cortex (M1) functional components in M1 gliomas enhances safe resection and reveals M1 plasticity potentials. Cancers 13 (15), 3808. doi:10.3390/cancers13153808.
Rossi, M., Sciortino, T., Conti Nibali, M., Gay, L., Viganò, L., Puglisi, G., Leonetti, A., Howells, H., Fornia, L., Cerri, G., Riva, M., Bello, L., 2021b. Clinical pearls and methods for intraoperative motor mapping. Neurosurgery 88 (3), 457–467. doi:10.1093/neuros/nyaa359.
Roux, F.E., Djidjeli, I., Durand, J.B., 2018. Functional architecture of the somatosensory homunculus detected by electrostimulation. J. Physiol. 596 (5), 941–956. doi:10.1113/JP275243.
Rozzi, S., Calzavara, R., Belmalih, A., Borra, E., Gregoriou, G.G., Matelli, M., Luppino, G., 2006. Cortical connections of the inferior parietal cortical convexity of the macaque monkey. Cereb. Cortex 16 (10), 1389–1417. doi:10.1093/cercor/bhj076.
Seki, K., Fetz, E.E., 2012. Gating of sensory input at spinal and cortical levels during preparation and execution of voluntary movement. J. Neurosci. 32 (3), 890–902. doi:10.1523/JNEUROSCI.4958-11.2012.
Schabrun, S.M., Ridding, M.C., Miles, T.S, 2008. Role of the primary motor and sensory cortex in precision grasping: a transcranial magnetic stimulation study. Eur. J. Neurosci. 27 (3), 750–756. doi:10.1111/j.1460-9568.2008.06039.x.
Simone, L., Fornia, L., Viganò, L., Sambataro, F., Rossi, M., Leonetti, A., Puglisi, G., Howells, H., Bellacicca, A., Bello, L., Cerri, G., 2020. Large scale networks for human hand-object interaction: Functionally distinct roles for two premotor regions identified intraoperatively. Neuroimage 204, 116215. doi:10.1016/j.neuroimage.2019.116215.
Simone, L., Viganò, L., Fornia, L., Howells, H., Leonetti, A., Puglisi, G., Bellacicca, A., Bello, L., Cerri, G., 2021. Distinct functional and structural connectivity of the human hand-knob supported by intraoperative findings. J. Neurosci. 41 (19), 4223–4233. doi:10.1523/JNEUROSCI.1574-20.2021.
Starr, A., Cohen, L.G., 1985. Gating' of somatosensory evoked potentials begins before the onset of voluntary movement in man. Brain Res. 348 (1), 183–186. doi:10.1016/0006-8993(85)90377-4.
Stepniewska, I., Gharbawie, O.A., Burish, M.J., Kaas, J.H., 2014. Effects of muscimol inactivations of functional domains in motor, premotor, and posterior parietal cortex on complex movements evoked by electrical stimulation. J. Neurophysiol. 111 (5), 1100–1119. doi:10.1152/jn.00491.2013.
Tadel, F., Baillet, S., Mosher, J.C., Pantazis, D., Leahy, R.M., 2011. Brainstorm: a user-friendly application for MEG/EEG analysis. Comput. Intell. Neurosci. 2011, 879716. doi:10.1155/2011/879716.
Turella, L., Rumiati, R., Lingnau, A., 2020. Hierarchical action encoding within the human brain. Cereb. Cortex 30 (5), 2924–2938. doi:10.1093/cercor/bhz284.
Umeda, T., Isa, T., Nishimura, Y., 2019. The somatosensory cortex receives information about motor output. Sci. Adv. 10 (7), eaaw5388. doi:10.1126/sciadv.aaw5388, 5.
Van Essen, D.C., Donahue, C., Dierker, D.L., Glasser, M.F., 2016. Parcellations and connectivity patterns in human and macaque cerebral cortex. In: Kennedy, H. (Ed.), Micro-, Meso- and Macro-Connectomics of the Brain. Springer, pp. 89–106.
Vesia, M., Bolton, D.A., Mochizuki, G., Staines, W.R, 2013. Human parietal and primary motor cortical interactions are selectively modulated during the transport and grip formation of goal-directed hand actions. Neuropsychologia 51 (3), 410–417. doi:10.1016/j.neuropsychologia.2012.11.022.
Viganò, L., Fornia, L., Rossi, M., Howells, H., Leonetti, A., Puglisi, G., Conti Nibali, M., Bellacicca, A., Grimaldi, M., Bello, L., Cerri, G., 2019. Anatomo-functional characterisation of the human "hand-knob": a direct electrophysiological study. Cortex J. Devoted Study Nervous Syst. Behav. 113, 239–254. doi:10.1016/j.cortex.2018.12.011.
Viganò, L, Howells, H, Fornia, L, Rossi, M, Conti Nibali, M, Puglisi, G, Leonetti, A, Simone, L, Bello, L, Cerri, G., 2021. Negative motor responses to direct electrical stimulation: Behavioral assessment hides different effects on muscles. Cortex 137, 194–204. doi:10.1016/j.cortex.2021.01.005.

Further reading

Rathelot, J.A., Strick, P.L., 2009. Subdivisions of primary motor cortex based on cortico-motoneuronal cells. Proc. Nat. Acad. Sci. U. S. A. 106 (3), 918–923. doi:10.1073/pnas.0808362106.
Viganò, L, Howells, H, Rossi, M, Rabuffetti, M, Puglisi, G, Leonetti, A, Bellacicca, A, Conti Nibali, M, Gay, L, Sciortino, T, Cerri, G, Bello, L, Fornia, L., 2021. Stimulation of frontal pathways disrupts hand muscle control during object manipulation. Brain doi:10.1093/brain/awab379, Epub ahead of print.